Sensitivity of the thermohaline circulation to tropical and high latitude freshwater forcing during the last glacial-interglacial cycle

Andreas Schmittner
School of Earth and Ocean Sciences, University of Victoria, Victoria, British Columbia, Canada

Amy C. Clement[1]
Lamont-Doherty Earth Observatory, Palisades, New York, USA

Received 20 September 2000; revised 8 August 2001; accepted 17 September 2001; published 10 May 2002.

[1] Recent studies indicate that the tropical freshwater budget of the Atlantic is modulated by changes in El Niño-Southern Oscillation (ENSO). If anomalies of the Atlantic freshwater balance persist on the order of decades, these might have a large influence on the North Atlantic thermohaline circulation (THC). Here we present a sensitivity study in which we use a model scenario for ENSO behavior during the last 120 kyr to force a simplified model of the THC with corresponding freshwater exchange between the tropical Atlantic and Pacific. If the steady state strength of the North Atlantic THC is similar to the present-day, its response to the forcing is of the order of 1–3 Sv (1 Sv = 10^6 m^3 s^{-1}). No mode changes of the THC are simulated for reasonable values of the coupling constant between freshwater exchange and ENSO. If, on the other hand, the steady state overturning is significantly weaker, a collapse of the THC occurs due to forcing from the tropics. The modeled THC variation due to tropical freshwater perturbations are compared to those resulting from middle- and high-latitude freshwater forcing due to long-term growth and decay of Northern Hemisphere ice sheets. It is found that both forcings are of similar amplitude except during the deglaciation when high latitude forcing dominates. A possible out-of-phase relationship between deep water formation in the North Pacific and North Atlantic is also explored. *INDEX TERMS:* 4267 Oceanography: General: Paleoceanography; 1620 Global Change: Climate dynamics (3309); 1635 Global Change: Oceans (4203); 1655 Global Change: Water cycles (1836); *KEYWORDS:* climate dynamics, oceans, water cycles, paleoceanography, numerical modeling, El Niño

1. Introduction

[2] It has long been recognized that the North Atlantic Ocean must have had a significant influence on global ice volume changes because of its role as a moisture source adjacent to the large Northern Hemisphere ice sheets [*Ruddiman and McIntyre*, 1981]. *Broecker and Denton* [1989] argued that changes in North Atlantic thermohaline circulation (THC) are an integral part of the glacial-interglacial swings in climate which are linked to changes in the Earth's orbital parameters. *Imbrie et al.* [1992] performed a comprehensive investigation into the mechanisms linking solar insolation changes at 65°N and ocean circulation with a near global array of paleoceanographic indicators. Their work provides geographical perspective on the progression of changes in the global ocean that are paced by the precessional and obliquity cycles. However, those authors were unable to identify the actual mechanism linking solar insolation with ocean circulation. Rather, they concluded that the initial response to orbital forcing must lay in the Arctic Ocean, where there are no long records. *Brickman et al.* [1999] perform ocean model experiments and show that the THC operates as a filter to Milankovic insolation changes. However, the direct impact of orbital changes on Atlantic THC over the last 3.2 Myr is small in their model. The link between orbital forcing and ocean circulation remains unclear.

[3] Evidence has accumulated that the North Atlantic THC might also have been actively involved in rapid climate fluctuations on millennial timescales during the last glaciation [*Bond et al.*, 1993; *Broecker*, 1997]. These studies generally point to the large ice sheets surrounding the North Atlantic during the last glaciation as a freshwater source available for triggering THC variations in the ultimate vicinity of the regions of deep water formation [see *Birchfield and Broecker*, 1990; *Alley et al.*, 1999]. From modeling studies it is known that the Atlantic THC is sensitive to freshwater perturbations [e.g., *Bryan*, 1986]. However, the origin of these meltwater pulses and their influence on North Atlantic Deep Water (NADW) is not clear from the observations [*Zahn et al.*, 1997; *Moore et al.*, 2000]. Thus, so far, the focus on processes triggering THC variability has been put at the high latitudes. See *Weaver et al.* [1999] for a review.

[4] Much less attention has been given to low-latitude processes, although the role of the tropics in high-latitude climate change has recently come into question [*Cane*, 1998; *Stocker*, 1998]. One process that may influence ocean circulation is the hydrological cycle. The surface freshwater budget of the Atlantic, which influences the strength of the THC [*Stocker and Wright*, 1991; *Rahmstorf*, 1996], is modulated by tropical atmospheric moisture transport across the Isthmus of Panama [*Weyl*, 1968]. *Latif et al.* [2000], using a coupled ocean-atmosphere general circulation model (GCM), and *Schmittner et al.* [2000], examining two reanalysis data sets, found that the surface freshwater balance of the tropical Atlantic Ocean is altered by tropical Pacific sea surface temperatures (SSTs). These results were confirmed by another recent work focusing on multidecadal variability [*Latif*, 2001]. The above studies suggest that during

[1]Now at Division of Meteorology and Physical Oceanography, Rosenstiel School of Marine and Atmospheric Science, University of Miami, Miami, Florida, USA.

Copyright 2002 by the American Geophysical Union.
0883-8305/02/2000PA000591$12.00

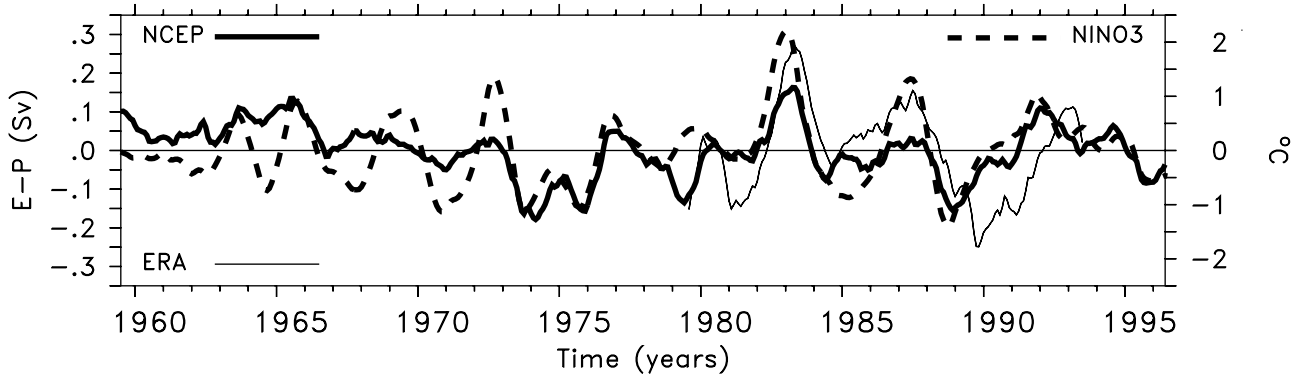

Figure 1. Tropical Atlantic freshwater balance $E-P$ (left axis) as a function of time from the NCEP (thick solid line) and ECMWF (thin solid line) reanalysis together with the NINO3 index (from NCEP; right axis, dashed line). A 12 month sliding window has been applied to the monthly data.

periods with warmer east Pacific SSTs (El Niño) atmospheric water vapor transport from the tropical Atlantic to the tropical Pacific is enhanced, leading to changes in atmospheric moisture convergence. Tropical freshwater perturbations induced by changes of ENSO can have a significant influence on the North Atlantic THC if the perturbations persist longer than a few decades [*Schmittner et al.*, 2000].

[5] In this paper, we explore how this oceanic link between the tropics and high latitudes may have operated under different orbital configurations during the last glacial cycle. *Clement et al.* [1999] used a simplified model of the tropical Pacific to show that orbitally driven changes in the seasonal cycle over the last 150 kyr exert a strong influence on the character of ENSO. They show that changes in ENSO behavior result in a mean sea surface temperature change that has an El Niño- or La Niña-like spatial pattern which varies on the timescale of the precessional cycle (21 kyr). Here we use the results of *Clement et al.* [1999] to explore how these orbitally driven changes in ENSO over the last 150 kyr would influence the high-latitude oceans.

2. Model Description and Forcing

[6] We use the zonally averaged ocean model from [*Wright and Stocker*, 1991] consisting of three basins representing the Pacific, Atlantic, and Indian connected through a zonally well mixed Southern Ocean. Each basin has constant longitudinal width of 140° (Pacific), 70° (Atlantic), and 75° (Indian), flat bathymetry, and coarse latitudinal resolution of ~10°. Further details about model geometry and resolution are described by *Stocker and Wright* [1996]. This model is coupled to a one-dimensional energy balance model of the atmosphere [*Stocker et al.*, 1992] including a simple representation of sea ice [*Wright and Stocker*, 1993] and an active meridional water vapor transport [*Schmittner and Stocker*, 1999]. Present-day seasonal forcing is applied as by *Schmittner and Stocker* [2001].

[7] The model is forced by the exchange of freshwater between the tropical Atlantic and Pacific. The freshwater flux anomaly (positive upward) in the Atlantic F_{fw} is taken proportional to the NINO3 index according to

$$F_{fw} = m\mathrm{NINO3}, \tag{1}$$

where m is the coupling constant (in Sv K^{-1}). The freshwater anomaly is equally distributed in the three equatorial boxes between 20°S and 20°N in the tropical Atlantic and is compensated at the same latitudes in the tropical Pacific.

[8] *Schmittner et al.* [2000] estimated the change of the total Atlantic freshwater balance due to a change in the Southern Oscillation Index (SOI) by one standard deviation to be 0.05 Sv. We have redone their analysis for the NINO3 index, which we will briefly describe in the following. Figure 1 shows the tropical Atlantic freshwater budget $E-P$ integrated over the Atlantic drainage basin from 20°S to 20°N for two reanalysis data sets together with the NINO3 index. Note the shorter length of the European Centre for Medium-Range Weather Forecasts (ECMWF) reanalysis compared to the National Centers for Environmental Prediction (NCEP) reanalysis, which reduces the significance of the analysis for the former. The correlation r and slopes m between the NINO3 and the tropical freshwater fluxes are $r = 0.62$ and $m = 0.065$ Sv K^{-1} for the NCEP reanalysis and $r = 0.55$ and $m = 0.074$ Sv K^{-1} for the ECMWF data set. A significant correlation at other latitudes has only been found between 20° and 40°N, where the correlation was negative in both data sets ($r = -0.4$ and $m = -0.017$ Sv K^{-1} for NCEP; $r = -0.35$ and $m = -0.018$ Sv K^{-1} for ECMWF). This suggests that the change in the total Atlantic freshwater budget for a change of the NINO3 index by 1°C is 0.048 Sv for NCEP and 0.056 Sv for ECMWF. Considering the uncertainties in the calculation of m, we perform runs with $m = 0.05$ Sv K^{-1} and $m = 0.1$ Sv K^{-1}, where we regard $m = 0.05$ Sv K^{-1} as the best estimate and $m = 0.1$ Sv K^{-1} as an upper limit. A more detailed description of the calculation of significance intervals and a discussion of the uncertainties and shortcomings can be found elsewhere [*Schmittner et al.*, 2000].

[9] As yet, there is no complete temporal reconstruction of the state of the tropical Pacific over the last glacial cycle. In particular, we are interested in how the east-west gradient in SST evolves over time since the preceding work points to this feature of the tropical climate as having a strong control over the longitudinal structure of the hydrological cycle. Modeling work by *Clement et al.* [1999] provides a plausible mechanism by which the east-west structure of the tropical Pacific is influenced by orbital forcing. Those authors generate a NINO3 index using the *Zebiak and Cane* [1987] coupled ocean-atmosphere model, which is forced by the solar insolation changes over the last 150 kyr. The model's active domain includes only the tropical Pacific (124°E–80°W, 29°N–29°S). It is an anomaly model, with some aspects of the oceanic and atmospheric physics linearized about the monthly climatology of the present. The main dynamics in the atmosphere and ocean are described by linear shallow water equations on an equatorial beta plane. In the ocean an additional shallow frictional layer of constant depth

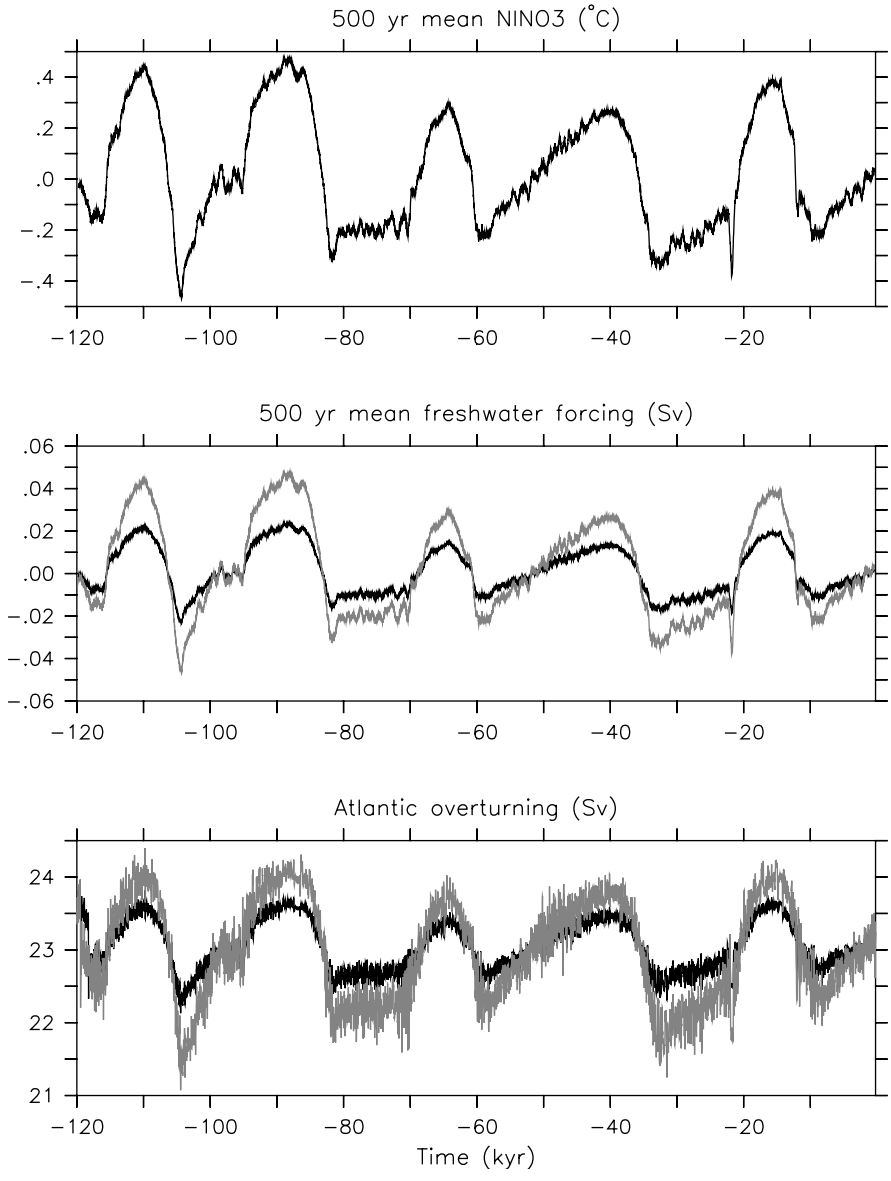

Figure 2. Time series of (top) NINO3 index, (middle) tropical freshwater forcing (positive values correspond to freshwater transfer from the Atlantic to the Pacific), and (bottom) response of the North Atlantic THC as annual mean maximum overturning below 1000 m depth. The black line corresponds to a small value for the coupling constant (m = 0.05 Sv K^{-1}; experiment LFHS; see (1) and Table 1), and the red line corresponds to a large value (m = 0.1 Sv K^{-1}; experiment HFHS). See color version of this figure at back of this issue.

(50 m) is included to account for the intensification of wind-driven currents near the surface. The ocean and atmosphere are coupled through a parameterization of the atmospheric heating which is computed from the SST anomaly, the specified background surface wind divergence field, and the modeled divergence anomaly. The Figure 2 (top) shows the resulting NINO3 SST anomaly for the last 120 kyr averaged over periods of 500 years. While the annual mean orbital forcing in the tropics is close to zero, there is a significant annual mean change in SST that varies on a precessional timescale. The mean change results from a change in the interannual variability with warm (cold) periods coinciding with more (less) frequent and larger (smaller) El Niño events. The change in ENSO behavior is driven by the orbitally induced changes in the seasonal cycle of solar radiation on the equator (see *Clement et al.* [1999] for a more complete description).

3. Model Response to ENSO-Induced Freshwater Forcing

[10] Figure 2 shows the tropical freshwater forcing and the response of the Atlantic THC in the standard model version. Increased freshwater export from the Atlantic to the Pacific during periods where the NINO3 index is positive (warm El Niño-like state) leads to increased salinities in the tropical Atlantic which are advected to the northern North Atlantic and cause enhanced deep water formation. For the best estimate value of m = 0.05 Sv K^{-1}

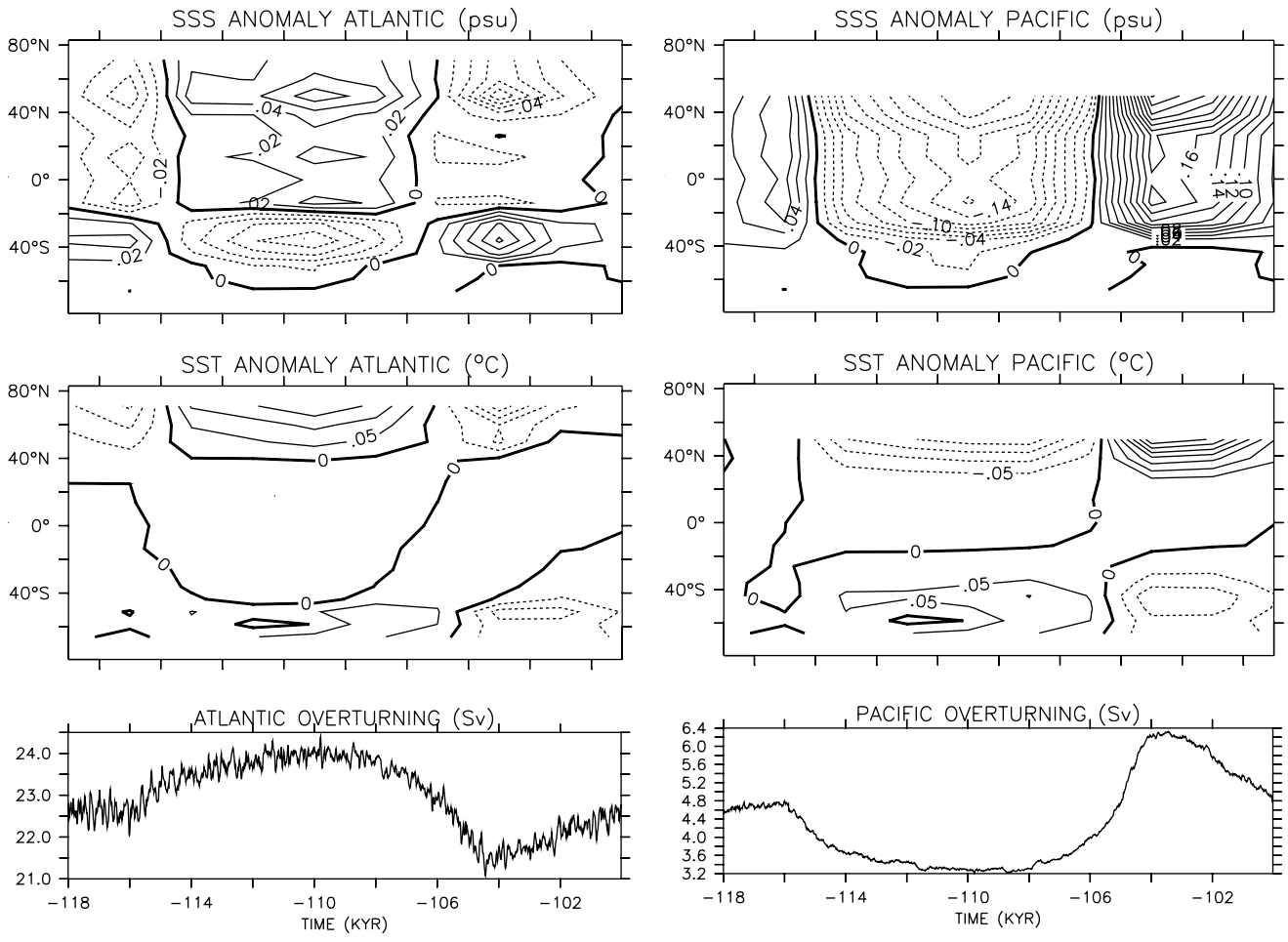

Figure 3. (top) Sea surface salinity and (middle) temperature anomalies (differences from time mean) for the (left) Atlantic and (right) Pacific Oceans as a function of time and latitude. The 100 year averages are plotted at the end of the averaging period with 2 kyr intervals. Isoline difference is 0.02 psu for SSS and 0.05°C for SST with negative values shown as dashed lines. (bottom) Time series of the annual mean maximum stream function below 1000 m depth in the corresponding basin for reference. Every tenth year is plotted.

the amplitude of the THC variations is small with only ∼1 Sv changes in overturning. The model response is approximately linear to the forcing reflecting the dominant precessional cycle of ∼20 kyr. The interannual variations in the forcing (not shown) are effectively eliminated through mixing of the freshwater anomalies during their travel from the tropics to high northern latitudes. The background variability is of decadal and centennial timescale. This background variability and the long-term (precessional) variations increase nearly linear if the coupling constant m is doubled.

[11] Next, we want to assess the signature of the model response in the surface properties of the Atlantic and Pacific Oceans. Since the signal is rather weak, we show results for $m = 0.1$ Sv K^{-1}. The values presented should be interpreted as the maximum signal with approximately linearly smaller response for smaller coupling constant m. Since the anomalies in the freshwater forcing are similar for each precessional cycle, we performed the sensitivity experiments below for the first cycle from 120 kyr BP to 100 kyr BP only. In Figure 3, salinity and temperature anomalies during the first precessional cycle are shown. As expected, during the period with more frequent El Niños around −110 kyr, the surface waters get saltier in the Atlantic north of 20°N and fresher in the Pacific, while during the period with more La Niña years around −104 kyr the Atlantic gets fresher and the Pacific gets saltier. Anomalies in the Pacific are ∼0.15 psu and reach maximum values of 0.2 psu in the North Pacific. In the Atlantic, anomalies ∼0.03 psu with maxima of 0.08 psu at 50°N are much smaller than in the Pacific.

[12] The different amplitudes in the Atlantic and Pacific are due to the different mean circulation patterns (see Figure 4 (top)) in these basins. In the Atlantic the tropical freshwater flux anomalies are advected northward and through the formation of NADW mixed into the deep ocean. In the Pacific where no deep water formation occurs, the tropical anomalies accumulate in surface and subsurface waters. While in the Pacific the salt anomalies have the same sign throughout the basin, in the Atlantic a dipole emerges with opposite signs north and south of 20°S. This dipole structure as well as the fact that the signal is larger at high latitudes and smaller in the tropics although the forcing is applied in the tropics is due to circulation changes as we show in the following.

[13] Figure 4 (bottom) shows the circulation during the El Niño phase around −110 kyr minus the the circulation during the La Niña phase around −104 kyr. Production of NADW is enhanced during the El Niño phase by ∼2.5 Sv compared to the La Niña phase, all of which exits the Atlantic into the Southern Ocean. The enhanced return flow of surface and subsurface waters leads to an increased freshwater inflow from the Southern Ocean to the South Atlantic, creating the negative salinity anomalies there. Increased advection of warm tropical waters to the north is also the reason for the warmer SSTs in the northern North Atlantic during the El Niño

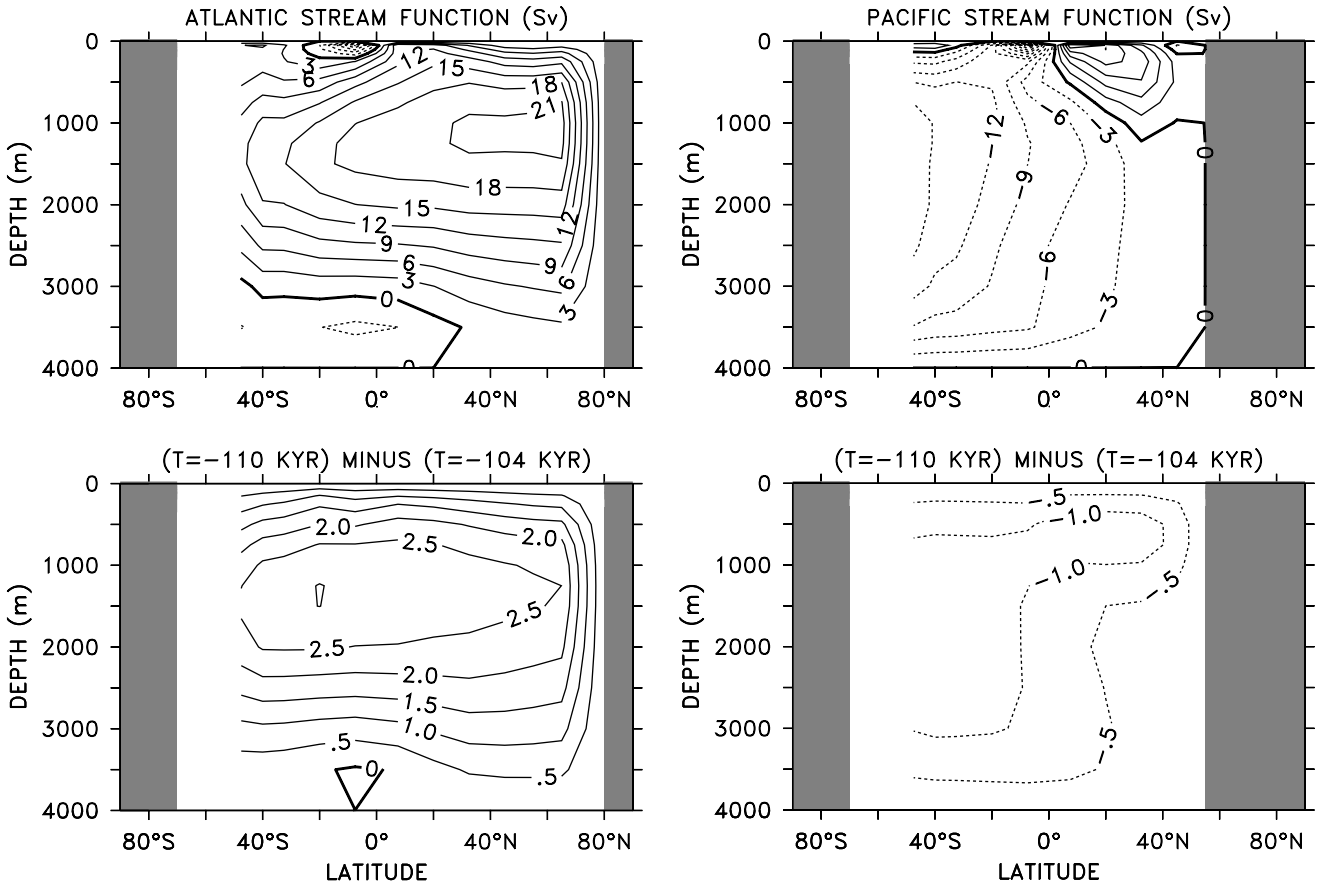

Figure 4. Stream function in the (left) Atlantic and (right) Pacific. Time mean state (top panels) is shown with isoline differences of 3 Sv. Difference in circulation between the states with maximum Atlantic overturning at −110 kyr B.P. and minimum overturning at −104 kyr B.P. (bottom panels) are drawn with isoline differences of 0.5 Sv.

phase (see Figure 3). In the North Pacific the formation of NPIW is reduced during El Niño periods, leading to colder and fresher conditions there. Generally, in this model version the response in the Atlantic and Pacific Oceans is in antiphase. In section 5 we will examine whether this out-of-phase response is robust and to what extent it is a consequence of the tropical freshwater forcing.

[14] In the experiments described above the influence of the tropical freshwater forcing on the THC was relatively small and therefore approximately linear to the forcing. However, we neglected all other influences on the THC during the last glacial-interglacial cycle. It is now generally believed that the production of NADW was substantially reduced during the Last Glacial Maximum (LGM). The reader is referred to *Boyle* [1995] for a review of the paleoproxy evidence and *Weaver et al.* [1998], *Ganopolski et al.* [1998], and *Winguth et al.* [1999] for modeling studies. As suggested by previous studies [*Stocker and Wright*, 1991; *Rahmstorf*, 1995], the influence of a given perturbation on the THC depends on the mean state of the THC itself and the fact that the same perturbation would have less of an impact when applied to a strong THC than when applied to a weak THC. Recent modeling studies [*Ganopolski and Rahmstorf*, 2002; *Schmittner et al.*, 2002] indicate that the sensitivity of the THC to a given perturbation is indeed largely increased if full glacial boundary conditions are applied. In order to test the influence of a different mean state on our model response, additional experiments have been performed in which we tuned the model such that the steady state THC is weaker. We produced two different additional steady states of the model: one with intermediate NADW formation rate and one with weak NADW formation rate.

[15] The tuning procedure is as follows. In the present model version the atmosphere is coupled to the ocean after an ocean spin-up in which SSTs and sea surface salinities (SSSs) are relaxed to observations. At the time of coupling, uncertain atmospheric parameters, like meridional eddy diffusivities, are diagnosed such that the steady state after coupling is close to the present-day climate. See *Stocker et al.* [1992] and *Schmittner and Stocker* [2001] for a detailed description of the coupling procedure. In order to get realistic deep water salinities the value of the relaxation SSS at the northern most box in the North Atlantic has been increased by 0.5 psu during the ocean spin-up in the standard model version. This value has been decreased to 0.3 psu in the intermediate NADW model version. For the weak NADW model version additionally, the parameterization of deep water formation along the slope of Antarctica has been modified. The rate of sea ice production which is used to form deep water in the southern ocean [see *Stocker and Wright*, 1996] was increased from 0.5 to 2 Sv to account for an increased Antarctic Bottom Water (AABW) production during the LGM. Note that owing to the coupling procedure described above these changes result in changes of atmospheric parameters.

[16] The Atlantic THC from the steady state of the intermediate and weak NADW model versions is shown in Figure 5. NADW formation decreased from ~23 Sv in the standard version (see Figure 4) to 19 Sv in the intermediate overturning version IO and to 16 Sv in the weak overturning version WO. AABW progres-

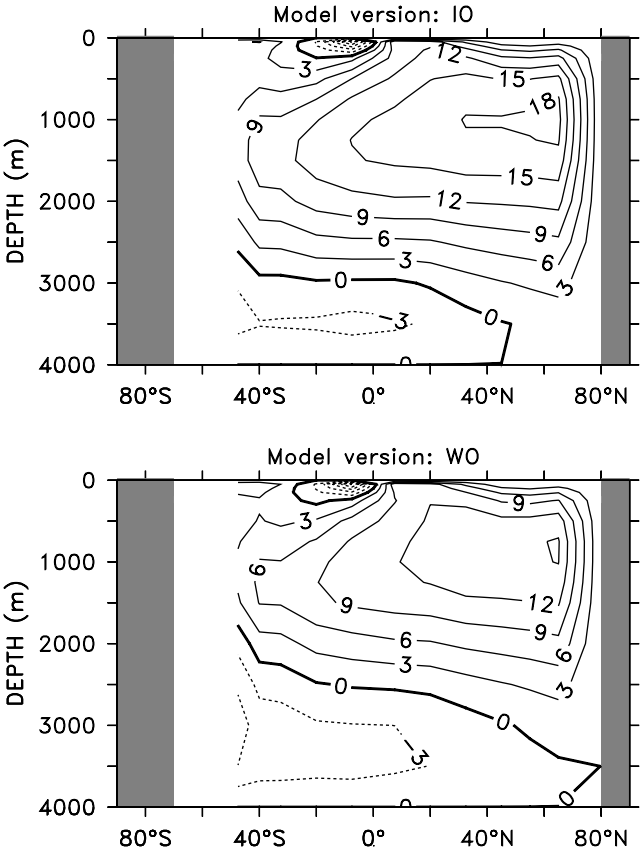

Figure 5. Annual mean steady state stream function in the Atlantic Ocean in Sv for the model versions with (top) intermediate NADW formation IO and (bottom) weak NADW formation WO. Isoline differences are 3 Sv.

sively moves north as NADW is weakened and eventually fills the entire basin below 2500 m in version WO. This is broadly consistent with $\delta^{13}C$ reconstructions of the circulation during LGM [*Duplessy et al.*, 1988] that show decreased and shallower NADW and a spreading of AABW farther north. Note that this should not be viewed as a simulation of LGM conditions since the air temperatures, SSTs, and SSSs are still close to present-day values. It is an attempt to examine the influence of the strength of the THC to a given forcing.

[17] In order to examine the dependence of the model response on the steady state strength of the Atlantic overturning in a general manner we repeated the experiments from *Schmittner et al.* [2000] (see their Figure 4) for the model versions with intermediate and weak overturning. Therefore freshwater was exchanged between the tropical Atlantic and Pacific at two different amplitudes, 0.02 and 0.04 Sv, which would correspond to a La Niña phase in the precessional cycle for the low and high coupling constant m = 0.05 Sv and m = 0.1 Sv, respectively (see Figure 2). The persistence time of the tropical freshwater perturbations was varied from 1 year to 100 years. Each experiment was integrated for 1000 years. The maximum response of the Atlantic overturning during the integration to these perturbations is shown in Figure 6 as a function of the persistence time. While for the smaller-amplitude perturbations the model version with intermediate overturning shows no mode changes of the THC even for long persistence times (100 years or more), the weak overturning version exhibits a breakdown of NADW formation for persistence times longer than 90 years. For the larger-amplitude perturbations (0.04 Sv) both model versions show a collapse of the North Atlantic THC for long persistence times. However, while for the weak overturning version a persistence time of 40 years is sufficient for a shutdown of NADW, in the version with intermediate overturning the circulation recovers for persistence times <80 years. This shows that not only the amplitude of a perturbation necessary for a breakdown of the Atlantic THC depends on the initial strength of the circulation but also the persistence time of such a perturbation. Further, these results demonstrate that the tropical forcing can induce mode changes of the THC.

4. Model Response to Freshwater Forcing due to Long-Term Variations of Northern Hemisphere Ice Sheets

[18] Here we want to examine the relative importance of the tropical freshwater forcing described above to high-latitude freshwater forcing. The surface freshwater balance of the Atlantic during the last glacial-interglacial cycle is likely to be influenced by the growth and decay of Northern Hemisphere ice sheets. In order to include this effect in the simplest possible manner we assume that the volume of freshwater trapped in Northern Hemisphere ice sheets is proportional to global sea level variations. This assumption is warranted since ice volume in the Southern Hemisphere contributed <20% to the global sea level changes between the Last Glacial Maximum and today [e.g., *Peltier*, 1998; *Clark et al.*, 2001, and references therein]. For the long-term variations of global sea level we use the stacked, smoothed oxygen isotope ($\delta^{18}O$) record from SPECMAP [*Imbrie et al.*, 1984]. We further assume that the surface freshwater flux anomaly in the North Atlantic F_{fw} is proportional to the temporal changes in Northern Hemisphere ice volume V_{NH}^{ice}. This leads to the following equation for the North Atlantic freshwater forcing:

$$F_{fw} = C\frac{\partial \delta^{18}O}{\partial t}, \tag{2}$$

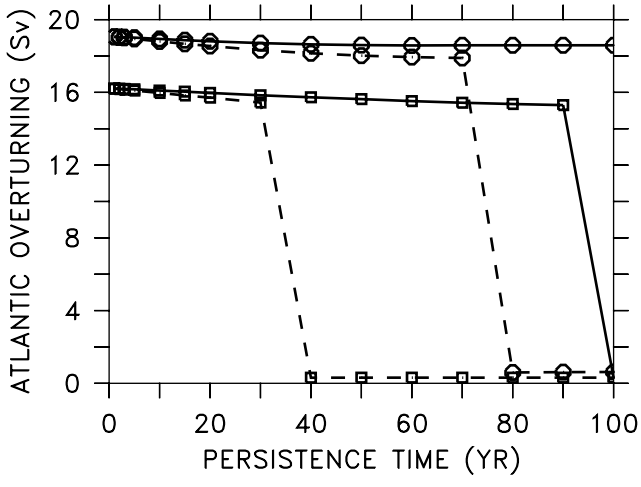

Figure 6. Maximum change in North Atlantic Deep Water formation rate as a response to stepwise tropical freshwater perturbations as a function of the persistence time of the perturbations. Circles correspond to the model version with intermediate overturning (IO), and squares denote the model version with weak overturning (WO). Different amplitudes of the forcing are used (0.02 Sv, solid lines; 0.04 Sv, dashed lines).

where C is a constant. In order to determine

$$C = 0.9\Delta V_{NH}^{\text{ice}} / \Delta\delta^{18}\text{O}, \quad (3)$$

where 0.9 arises from the different densities of water and ice, we use estimates for Northern Hemisphere ice volume changes between the LGM and present-day $\Delta V_{NH}^{\text{ice}}$ and the appropriate value for $\Delta\delta^{18}\text{O} = 4$. *Berger et al.* [1998] report a relatively high value of $\Delta V_{NH}^{\text{ice}} = 50 \times 10^6$ km^3 (corresponding to a 125 m global sea level drop) in a transient coupled ice sheet climate model study. A lower value of $\Delta V_{NH}^{\text{ice}} = 25 \times 10^6$ km^3 is based on steady state simulations of an ice sheet model with realistic bed properties [*Licciardi et al.*, 1998] in which the volume of the Laurentide ice sheet was estimated to be around 20×10^6 km^3 and a crude estimation of the smaller ice sheets of 5×10^6 km^3. These values for $\Delta V_{NH}^{\text{ice}}$ lead to $C = 1.13 \times 10^7$ km^3 and $C = 0.57 \times 10^7$ km^3, respectively. The total freshwater flux anomaly F_{fw} is equally distributed in the North Atlantic boxes northward of 20°N. Note that the spatial distribution of the freshwater anomalies does not affect the model response qualitatively. However, the greater the portion of the total anomaly supplied near the regions of deep water formation, the larger the efficiency of the anomaly [*Rahmstorf*, 1996].

[19] In the above approach, it is also assumed that the moisture source of the Northern Hemisphere ice sheets is by and large the Atlantic and that most part of the meltwater and calving ice bergs from the ice sheets enter the North Atlantic drainage basin. These assumptions are strong simplifications since it is likely that at least the western part of the Laurentide ice sheet was supplied with moisture from the Pacific and also lost freshwater to the east Pacific through calving and melting. Note, however, that qualitatively, our results do not depend on these assumptions. If the relative role of the Atlantic in changes of the Northern Hemisphere ice sheet's moisture balance would have been smaller, this could be accounted for with a smaller value of C. In the present study, however, we do not consider changes in the Pacific surface freshwater balance due to variations of Northern Hemisphere ice sheets.

[20] In Figure 7 the resulting freshwater forcing of the Atlantic and the model response are shown. Global mean salinity changes accordingly to the implied global sea level. The difference in global mean salinity between present-day and the LGM is about 1 (0.5) psu for $C = 1.13 \times 10^7$ km^3 ($C = 0.57 \times 10^7$ km^3). North Atlantic overturning increases during ice growth phases (e.g., around -150 kyr and -70 kyr) and decreases during melting phases. Ice growth leads to an extraction of freshwater from the North Atlantic. This increases salinity and density of near surface water masses leading to stronger overturning. Figure 7 can be directly compared to Figure 2 since the same model version was used. Generally, the freshwater forcing due to ice sheet variations is somewhat larger than the tropical anomalies due to changes in ENSO. For the lower value of C and the most part of the simulation with the larger C the response of the Atlantic THC to the forcing is approximately linear (except for some minor jumps). The amplitude of these linear changes is $\sim$2 Sv for $C = 1.13 \times 10^7$ km^3 and 4 Sv for $C = 0.57 \times 10^7$ km^3 and therefore similar to the response to the ENSO induced changes (1–3 Sv; see Figure 2).

[21] However, the overturning collapses for the large value of C during the last deglaciation around 16 kyr B.P. This is consistent with other model studies concerning large meltwater input into the North Atlantic during the last deglaciation [e.g., *Manabe and Stouffer*, 1995; *Fanning and Weaver*, 1997] but also with evidence from climate proxy records [e.g., *Dansgaard et al.*, 1989; *Venz et al.*, 1999; *Rühlemann et al.*, 1999].

[22] The sensitivity of the Atlantic THC to the forcing would be increased for the model versions with an intermediate or weak steady state overturning similarly to the results presented in section 3.1. Since, for example, a tropical freshwater perturbation

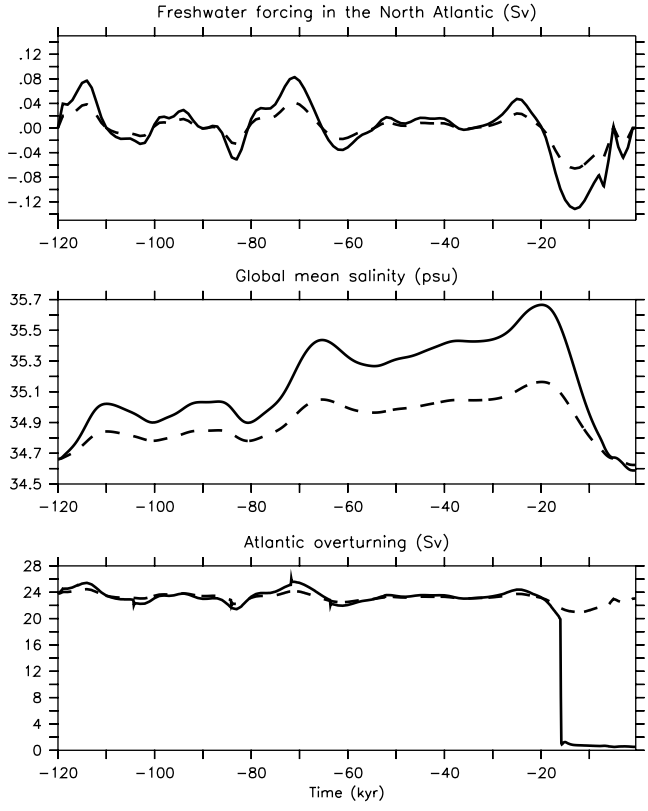

Figure 7. (top) Evolution of high-latitude freshwater forcing (positive upward) due to Northern Hemisphere continental ice volume changes calculated as the time derivative of the stacked, smoothed δ^{18}O record from SPECMAP (see (2)). Model response of (middle) global mean salinity and (bottom) Atlantic overturning for different values of $C = 1.13 \times 10^7$ km^3 (solid line) and $C = 0.57 \times 10^7$ km^3 (dashed line).

of 0.04 Sv persisting longer than 80 years is sufficient to shut down NADW in the intermediate overturning model version (see Figure 6), we would expect that in this model version, NADW formation stops during the last deglaciation even for the lower value of $C = 0.57 \times 10^7$ km^3.

[23] Note that no clear phase relation between the tropical and high-latitude forcings is present. However, analysis of lagged correlation shows that high-latitude forcing leads the ENSO forcing by $\sim$5–6 kyr. It is not surprising that there exists some relation between the two signals because they are both caused by the orbitally driven variations in insolation. A linear combination of the two forcings would lead to mutual amplifications around -114 kyr B.P., -105 kyr B.P., -94 kyr B.P., -80 kyr B.P., -67 kyr B.P., -60 kyr B.P., -42 kyr B.P., and -10 kyr B.P.

5. North Pacific Ventilation Changes

[24] Present-day conditions in the North Pacific differ largely from those in the North Atlantic. While in the North Atlantic, sea surface salinities are relatively large (around 34.9 psu) and deep waters are well ventilated, the North Pacific is fresh (32.5 psu), and no deep water is formed [*Warren*, 1983; *Weaver et al.*, 1999]. However, subsurface properties in the North Pacific have varied on numerous timescales [e.g., *Behl and Kennett*, 1996]. Some sediment records suggest antiphase ventilation patterns between the North Pacific and the North Atlantic during the last deglaciation [*van Geen et al.*, 1996], and it has been speculated whether they are

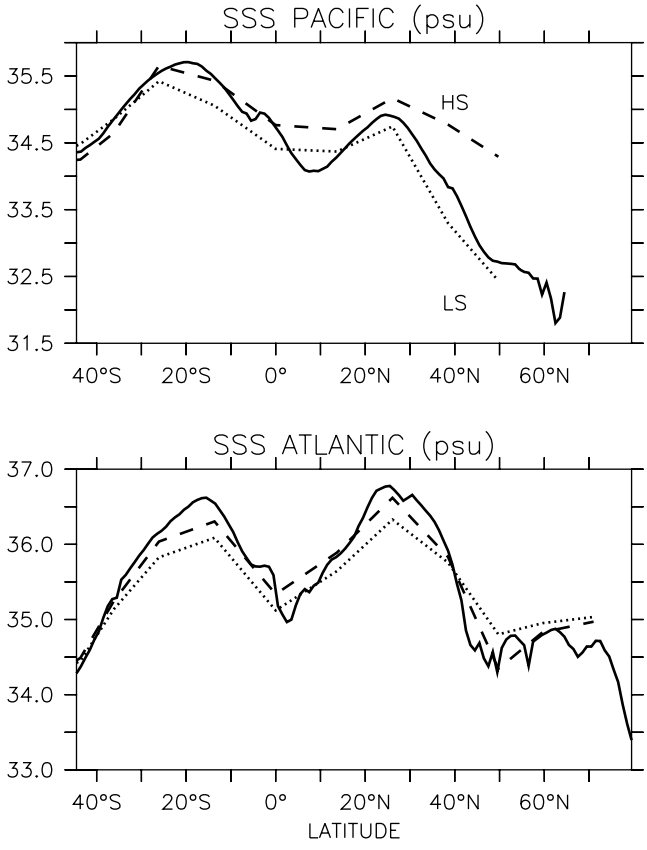

Figure 8. Annual mean sea surface salinities in the (top) Pacific and (bottom) Atlantic Oceans of the steady states from two model versions and present-day observations [*Levitus et al.*, 1994]. Dashed lines correspond to a version with high North Pacific salinity (HS), dotted lines to a version with low North Pacific salinity (LS), and solid lines to the zonally averaged observations.

caused by variations in the tropical Atlantic to Pacific freshwater exchange [*Zheng et al.*, 2000].

[25] In this section we will focus on how changes in both the tropics and in the North Atlantic may influence circulation changes in the North Pacific. First, we examine model runs in which the circulation changes are approximately linear to the tropical freshwater forcing. Subsequently, we will investigate the model response in the North Pacific to rapid changes of the Atlantic THC.

5.1. Linear Circulation Changes

[26] In the present-day climate, ventilation of deep northern North Pacific waters is prevented by the strong halocline [*Warren*, 1983]. In the standard model version used above, surface salinities in the northern North Pacific are up to 1.5 psu larger than zonally averaged observations from *Levitus et al.* [1994] (see Figure 8), leading to a stratification that is too weak. Therefore we tuned model parameters in order to get more realistic salinities there. In the present model version the ratio of precipitation into the different basins p_n and the zonal mean precipitation P is constant $c_n = p_n/P$ [*Schmittner and Stocker*, 1999]. We changed the ratio c_n in the two northernmost boxes in the North Pacific such that more precipitation is distributed into the North Pacific. In order to conserve precipitation the values of c_n at the corresponding latitudes in the Atlantic have been changed accordingly. This has the desired effect of lowering North Pacific SSS to approximately the observed values as shown in Figure 8, while the surface properties elsewhere and Atlantic overturning rates (increased by 2 Sv) are similar. The largest difference between the circulation patterns of these two model versions is found in the vertical extent of the meridional overturning cell of the North Pacific (not shown), which in the low North Pacific salinity version is shallower than 500 m (compared with 1000 m depth in the high North Pacific salinity version), while its strength increased only sightly from 15.8 to 17.6 Sv.

[27] In Figure 9 the maximum meridional heat flux in the Pacific during the precessional cycle from 120 to 100 kyr B.P. is shown for different model versions listed in Table 1. This is a measure of the intensity of the meridional overturning cell in the North Pacific, which in our model is closely related to North Pacific Intermediate Water (NPIW) formation. In the standard model experiments discussed above (high forcing, high salinity (HFHS)) the maximum meridional heat flux in the Pacific shows changes of ~10% between the El Niño phase and the La Niña phase. In the model version with lower SSS in the North Pacific (experiment HFLS) northward heat flux in the North Pacific is more than one third smaller than in the high North Pacific salinity version. It is approximately constant and shows no response to the forcing. This leads to the conclusion that the North Pacific-North Atlantic antiphase response discussed above depends on North Pacific SSS. In a model version with low northern North Pacific SSS (exp. HFLS in Figure 9) and a strong halocline in the northern North Pacific, similar to the present-day climatology, NPIW does not respond to the tropical freshwater forcing. If northern North Pacific SSSs are larger (experiment HFHS in Figure 9) with a corresponding weaker halocline, then an antiphase relation between NPIW and NADW formation is possible. Note that the SSS anomalies (not shown) during the precessional cycle are similar to the ones for the high North Pacific salinity version shown in Figure 3 except that the maximum of the anomalies in the Pacific is now located at low latitudes. SST anomalies in the Pacific are negligible in experiment HFLS, while in the Atlantic they are similar to the ones of experiment HFHS.

[28] Similar antiphase ventilation changes have previously been found in different model studies with simplified ocean-atmosphere models [*Wright and Stocker*, 1993] and also with fully coupled ocean-atmosphere GCMs [*Mikolajewicz et al.*, 1997]. In these studies a breakdown of the Atlantic thermohaline circulation induced by North Atlantic freshwater perturbations leads to a cooling of Northern Hemisphere surface air temperatures, which also cools North Pacific surface waters, increasing their densities such that NPIW formation increases. Here our freshwater forcing

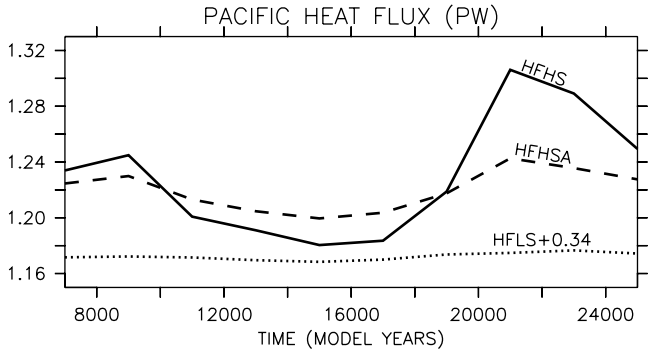

Figure 9. Maximum meridional heat flux in petawatts (1PW = 10^{15}W) in the Pacific for different model versions listed in Table 1. For model version HFLS, 0.34 PW has been added for axis scaling convenience. Note that the time axis is in model years. To convert into years B.P., subtract 125 kyr.

Table 1. Abbreviations Used for the Sensitivity Experiments[a]

	m, Sv K^{-1}	SSS NP	Basin[b]	Atlantic Overturning,[c] Sv
LFHS	0.05	high (34.3 psu)	Atlantic and Pacific	23.0
HFHS	0.1	high (34.3 psu)	Atlantic and Pacific	23.0
HFHSA	0.1	high (34.3 psu)	Atlantic only	23.0
HFLS	0.1	low (32.4 psu)	Atlantic and Pacific	24.6
HS	...	high (34.3 psu)	Atlantic and Pacific	23.0
HSA	...	high (34.3 psu)	Atlantic only	23.0
LS	...	low (32.4 psu)	Atlantic and Pacific	24.6
VLS	...	very low (31.6 psu)	Atlantic and Pacific	24.9

[a] Here m denotes the coupling constant between the NINO3 index and Atlantic to Pacific freshwater exchange (see (1)). SSS NP denotes the SSS of the steady state in the northern North Pacific.
[b] The basins to which the freshwater forcing is applied are listed.
[c] Atlantic overturning denotes the strength of the NADW formation rate in the steady state.

affects tropical SSS in the Pacific directly which, after being transported to the high northern latitudes, can induce changes in NPIW formation. In order to address the question to what extent the ventilation changes in the North Pacific seen in experiment HFHS are a direct effect of the applied tropical forcing or merely a response to changes in the Atlantic we performed an additional experiment where the freshwater forcing was only applied in the Atlantic (experiment HFHSA). Since no compensation in the Pacific occurs, global mean salinity changes in this experiment. As shown in Figure 9, in this case, the meridional heat flux changes are only one third of the amplitude of those found in the experiment where the forcing was also applied to the Pacific. This leads to the conclusion that most of the change (two thirds) in NPIW formation seen in the standard experiment (HFHS) is a direct response to the freshwater forcing in the tropical Pacific, while only a smaller part (one third) is due to changes in the Atlantic circulation.

5.2. Rapid Circulation Changes

[29] In order to extend the discussion of North Pacific circulation changes to cases where a breakdown of the Atlantic THC occurs we performed additional sensitivity experiments in which such a collapse was forced by tropical freshwater perturbations in different model versions. We exchanged 0.5 Sv from the tropical Pacific into the tropical Atlantic for 100 years. This is a much stronger freshwater forcing than applied in the previous sections and is sufficient to force a breakdown of the Atlantic THC. In Figure 10 the maximum meridional heat fluxes in the Atlantic and Pacific are shown for different model versions (see Table 1).

[30] In the high North Pacific salinity version (HS) the breakdown of the Atlantic THC is accompanied by increased ventilation in the North Pacific, which results in an increase of the maximum meridional heat flux by nearly 0.5 PW during the first 100 years of the experiment. For the next 900 years the circulation in the Pacific shows a slight further increase to an equilibrium value of $\sim$1.5 PW. In order to examine how much of these changes are a direct consequence of the tropical freshwater forcing in the Pacific or merely a response to the changes in the Atlantic THC a simulation was performed in which only the Atlantic was forced (HSA) similar to experiment HFHSA in section 5.1. In this case the circulation in the North Pacific increases less strongly during the first 100 years, but the equilibrium changes are very similar. This indicates that in contrast to the linear changes discussed in section 5.1, a breakdown of the Atlantic THC is the major forcing mechanism for the North Pacific circulation changes and not the direct tropical freshwater forcing. The reason here is that cooling of North Atlantic SSTs and northern high latitude air temperatures is much larger if the Atlantic THC experiences a complete shutdown compared to the case when it is only weakened. Cooler air temperatures cause colder SSTs in the North Pacific via air-sea heat exchange, decrease the stability of the water column, and lead to increased ventilation in the North Pacific.

[31] Similar to the simulations in section 5.1, the response in the North Pacific is strongly dependent on northern North Pacific SSS in the steady state. For the low North Pacific salinity version (LS) the circulation changes in the Pacific are much smaller than for version HS. If the salinity in the North Pacific is reduced even further to "very low salinities" (version VLS), the response is largely suppressed in the North Pacific. Note that the spin down time of the Atlantic THC is also dependent on North Pacific SSS. The shutdown of the Atlantic THC leads to a strong cooling of high northern latitude surface air temperatures (SATs). This is a negative feedback for the spin down of the Atlantic THC since it decreases North Atlantic SSTs and therefore increases surface water densities. Increased North Pacific meridional heat flux, on the other hand, tries to damp the cooling of high northern SATs and hence weakens the negative feedback and therefore weakens the stability of the Atlantic THC. The stronger the stratification in the North Pacific the less Pacific meridional heat flux increases as a response to the changes in the Atlantic. This results in an increased stability of Atlantic THC as can be seen in the longer spin down timescale for versions with lower North Pacific SSS in Figure 10.

[32] The equilibrium stream function in the Pacific Ocean after the breakdown of the Atlantic THC is shown in Figure 11. In version HS, surface waters in the northern North Pacific downwell to intermediate depths between 1000 and 2000 m at a rate of 18 Sv. Most of this water upwells in the North Pacific and interhemispheric transport is small. Note that this circulation is fundamentally different from that of the present-day Atlantic since it is confined to the North Pacific and does not set up a global circulation with interbasin water exchange. In version LS, North Pacific meridional overturning is much shallower compared with version HS.

6. Summary and Discussion

[33] We have presented a plausible mechanism by which variations of the orbital parameters cause changes in the formation of deep water in the North Atlantic. This mechanism involves orbitally driven changes in ENSO, which alter the tropical Atlantic freshwater balance. The tropical freshwater perturbations are advected to the regions of deep water formation and lead to changes of the rate of NADW production. For a quantitative assessment of this mechanism an idealized model of the THC was forced with tropical freshwater exchange between the Atlantic and Pacific Oceans. Variations of the NINO3 index on precessional timescales ($\simeq$21 kyr) with an amplitude of about $\pm$0.4°C result in tropical Pacific-Atlantic freshwater exchange of $\pm$0.02 to $\pm$0.04 Sv. This leads to changes in the Atlantic THC of 1–3 Sv. These changes are considerably larger than those found by *Brickman et al.* [1999], who used the direct orbital forcing. The picture we advance here is very different from that of *Imbrie et al.* [1992]. Those authors argued that insolation changes at 65°N initially influence water mass formation in the Arctic ocean, which

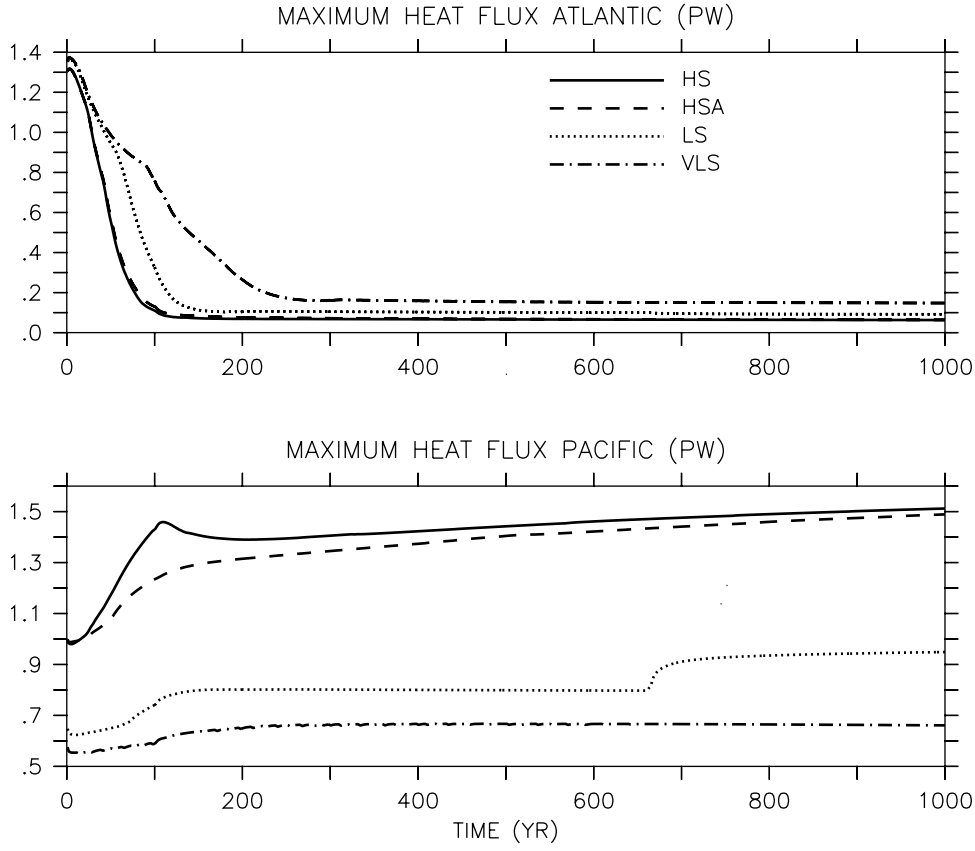

Figure 10. Annual mean maximum meridional heat fluxes in the (top) Atlantic and (bottom) Pacific for different model versions listed in Table 1. The model was forced with a strong (0.5 Sv) stepwise (100 year) tropical freshwater exchange from the Pacific to the Atlantic, which leads to a shut down of Atlantic deep water formation.

is seen first in proxies from the Southern ocean and equatorial region, and then later in the North Atlantic.

[34] The model used in this study lacks atmospheric dynamics and zonal resolution. However, it has been extensively tested, and the response to freshwater forcing is similar to three-dimensional GCMs. The model is suitable for integrations on glacial-interglacial timescales, which is not possible with fully coupled GCMs. We concentrated on freshwater forcing induced by changes in ENSO and Northern Hemisphere ice sheets and neglected other forcings, such as atmospheric CO_2 concentration, ice sheets, vegetation, or solar insolation. Hence the aim of this study was not a realistic simulation of the THC variations during the last glacial-interglacial cycle. We note that this mechanism only operates on a precessional timescale. The 100 kyr cycle in global ice volume and ocean proxies, and the link with eccentricity is currently unexplained. However, it is known that the strength of the THC has varied with the large climatic changes during the last glacial-interglacial. Thus we performed sensitivity experiments with different circulation strengths. For a weaker THC the tropical freshwater perturbations are sufficient to trigger rapid mode changes. An increased sensitivity of a weaker THC would apply not only to tropical freshwater forcing but also to high-latitude forcing. This raises the possibility that changes in the strength of the Atlantic THC are the amplifier for rapid climate changes seen during the last glacial period. Since recent modeling studies indicate increased sensitivity of the THC under full glacial boundary conditions [*Ganopolski and Rahmstorf*, 2001; *Schmittner et al.*, 2002], it is desirable that the present study is repeated with a more realistic glacial background climate.

[35] As a first step to assess the relative importance of the ENSO-induced freshwater forcing to high-latitude freshwater forcing on an orbital timescale, the effect of long-term changes of the Northern Hemisphere ice sheets on the North Atlantic freshwater balance has been considered. Therefore the stacked, smoothed $\delta^{18}O$ record from SPECMAP was used as a measure for North Atlantic freshwater forcing. A comparison of these two forcing mechanisms and the model responses to them suggests that except for the last deglaciation, the two forcing mechanisms are of similar magnitude, though the high-latitude forcing is somewhat stronger. Therefore we conclude that the tropics might have significantly contributed to THC variations during the last glacial-interglacial cycle. However, during the last deglaciation, high-latitude forcing clearly dominates.

[36] Once the THC is collapsed in our model, it remains in that state. The stability of the state without NADW formation in our model, while consistent with coupled GCM results [*Manabe and Stouffer*, 1999], is presumably not realistic and is most probably due to the absence of feedbacks which would destabilize this state. One such mechanism is the reduced runoff from the continents associated with a cooling around the North Atlantic [*Wright and Stocker*, 1993]. This would lead to increased snow and ice accumulation on land and therefore reduced freshwater input into the North Atlantic. Other possible effects destabilizing the steady state without NADW formation are associated with the dynamical response of the atmosphere [*Schiller et al.*, 1997; *Fanning and Weaver*, 1997] or with an increased freshwater export out of the Atlantic drainage basin in a state with no NADW formation [*Lohmann et al.*, 2001], which are also neglected in our model. Although it is possible to

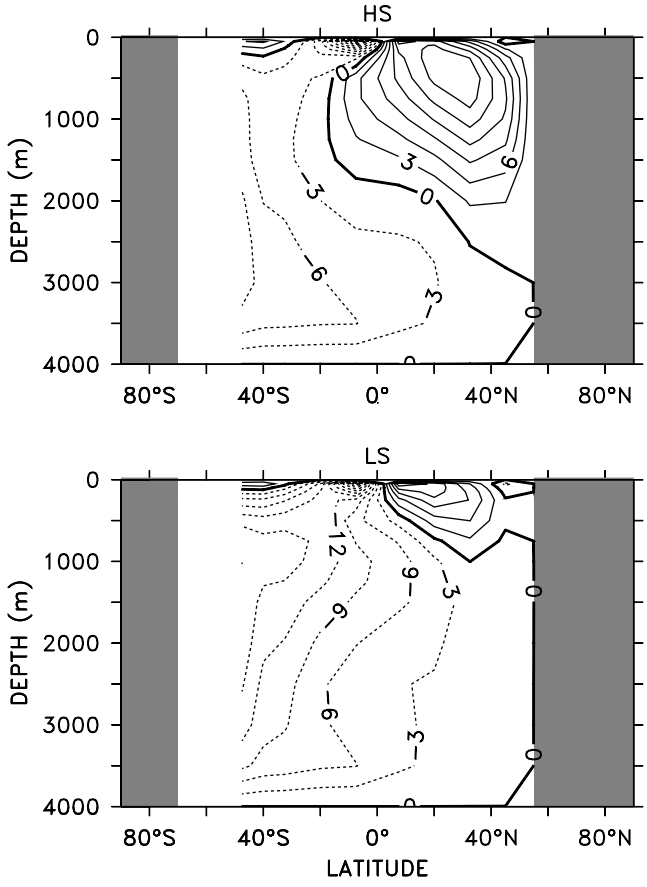

Figure 11. Annual mean steady state overturning in the Pacific Ocean after the breakdown of the Atlantic THC. In the high North Pacific salinity model version (top panel), increased downwelling in the North Pacific occurs, while for the low North Pacific salinity version (bottom panel) the ventilation changes are much smaller.

parameterize these effects we decided not to do so since we did not attempt to simulate realistic variations of the THC during the last glacial-interglacial cycle. Rather, we wanted to examine if a particular forcing can induce mode changes or not.

[37] The model response in the North Pacific is highly dependent on the steady state stratification in the northern North Pacific. For weak stratification (or high SSS), tropical freshwater forcing can induce changes in NPIW formation in antiphase to ventilation changes in the North Atlantic. A breakdown of the Atlantic THC can also lead to increased NPIW formation in case of weak stratification via atmospheric cooling. Increased meridional heat flux in the North Pacific due to increased NPIW formation causes reduced cooling of high northern latitude air temperatures and, via air-sea heat exchange, reduced cooling of North Atlantic SSTs. This has a further destabilizing effect on the THC in the North Atlantic. If northern North Pacific stratification is larger (low SSS) and more consistent with present-day observations, the response of NPIW formation to both the direct tropical forcing and the changes in the Atlantic THC is much weaker.

[38] The processes thought to be responsible for the formation of NPIW in the real world [e.g., *Talley*, 1993; *Yasuda*, 1997] are unlikely to have a good representation in our zonally averaged model. Particularly, all changes in wind stress have been neglected, which are probably important [*Mikolajewicz et al.*, 1997]. However, the response to the thermal and freshwater forcing on the largest spatial scales should be captured by the model and is at least qualitatively consistent with results from three-dimensional GCMs [*Rahmstorf*, 1995; *Mikolajewicz et al.*, 1997].

[39] The use of the model results of *Clement et al.* [1999] to derive tropical freshwater forcing is a vast simplification of how the tropical hydrological cycle may change on glacial-interglacial timescales. In particular, orbitally driven changes in the monsoon circulation are likely to be important and are not included in the scenario advanced here. There is also likely to be some feedback between high-latitude and tropical climate change which is not taken into account here. For example, as ice builds at high latitudes, the equator to pole temperature gradient would increase, which would alter the mean winds and have a potentially strong impact on the tropical coupled system [e.g., *Bush and Philander*, 1998]. The modeling studies by *Hostetler and Mix* [1999] and *Lohmann and Lorenz* [2000] suggest that glacial tropical SSTs lead to a net loss of fresh water from the Atlantic basin. Clearly, the tropical hydrological cycle will be affected by both the full orbital forcing and the glacial-interglacial changes in high-latitude climate. Further work is necessary to evaluate this.

[40] While the scenario we present here is subject to a certain number of caveats, it highlights the potential influence of the tropics on high-latitude ocean circulation. We have shown that orbitally induced ENSO-related freshwater perturbations in the tropics could have significantly influenced deep and intermediate water production at high northern latitudes during the last glacial-interglacial cycle. Paleoceanographic records are becoming available which provide a more detailed view of the evolution of the tropical oceans on this timescale [e.g., *Lea et al.*, 2000]. Further modeling and observational work is necessary to explore the link between the low and high latitudes over glacial cycles.

[41] **Acknowledgments.** We appreciated comments from A. J. Weaver and two anonymous reviewers. SPECMAP $\delta^{18}O$ data have been provided by *Imbrie et al.* [1989] SPECMAP Archive 1. IGBP PAGES/World Data Center-A for Paleoclimatology Data Contribution Series 90-001. NOAA/NGDC Paleoclimatology Program, Boulder, Colorado, USA, available at ftp://ftp.ngdc.noaa.gov/paleo/paleocean/specmap/specmap1. Reanalysis data sets were provided by the NOAA Climate Diagnostics Center (http://www.cdc.noaa.gov/) and by the European Centre for Medium Range Weather Forecast. This study was supported by NSERC strategic grant STP0192999 and the NSERC Climate System History and Dynamics Project. ACC was supported by NSF Grant ATM99-86515.

References

Alley, R. B., P. U. Clark, L. D. Keigwin, and R. S. Webb, Making sense of millennial-scale climate change, in *Mechanisms of Global Climate Change at Millennial Time Scales*, *Geophys. Monogr. Ser.*, vol. 112, edited by P. U. Clark, R. S. Webb, and L. Keigwin, pp. 385–394, AGU, Washington, D. C., 1999.

Behl, R., and J. Kennett, Brief interstadial events in the Santa Barbara Basin, NE Pacific during the past 60 kyr, *Nature*, *379*, 243–246, 1996.

Berger, A., M.-F. Loutre, and H. Gallée, Sensitivity of the LLN climate model to the astronomical and CO_2 forcings over the last 200 ky, *Clim. Dyn.*, *14*, 615–629, 1998.

Birchfield, G. E., and W. S. Broecker, A salt oscillator in the glacial Atlantic?, 2, A "scale analysis" model, *Paleoceanography*, *5*, 835–843, 1990.

Bond, G., W. S. Broecker, S. J. Johnsen, J. McManus, L. Labeyrie, J. Jouzel, and G. Bonani, Correlations between climate records from North Atlantic sediments and Greenland ice, *Nature*, *365*, 143–147, 1993.

Boyle, E. A., Last-Glacial-Maximum North Atlantic Deep Water: On, off or somewhere in-between?, *Philos. Trans. R. Soc. London, Ser. B*, *348*, 243–253, 1995.

Brickman, D., W. Hyde, and D. G. Wright, Filtering of Milankovitch cycles by the thermohaline circulation, *J. Clim.*, *12*, 1644–1658, 1999.

Broecker, W. S., Thermohaline circulation, the Achilles heel of our climate system: Will man-made CO_2 upset the current balance?, *Science*, *278*, 1582–1588, 1997.

Broecker, W. S., and G. H. Denton, The role of

ocean-atmosphere reorganizations in glacial cycles, *Geochim. Cosmochim. Acta*, *53*, 2465–2501, 1989.

Bryan, F., High-latitude salinity effects and interhemispheric thermohaline circulations, *Nature*, *323*, 301–304, 1986.

Bush, A., and S. Philander, The role of ocean-atmosphere interactions in tropical cooling during the Last Glacial Maximum, *Science*, *279*, 1341–1344, 1998.

Cane, M. A., A role for the tropical Pacific, *Science*, *282*, 59–60, 1998.

Clark, P. U., A. C. Mix, and E. Bard, Ice sheets and sea level of the Last Glacial Maximum, *EOS Trans. AGU*, *82*, 241–247, 2001.

Clement, A. C., R. Seager, and M. A. Cane, Orbital controls on the El Niño/Southern Oscillation and the tropical climate, *Paleoceanography*, *14*, 441–456, 1999.

Dansgaard, W., J. W. C. White, and S. J. Johnsen, The abrupt termination of the Younger Dryas climate event, *Nature*, *339*, 532–534, 1989.

Duplessy, J.-C., N. J. Shackleton, R. G. Fairbanks, L. Labeyrie, D. Oppo, and N. Kallel, Deepwater source variations during the last climate cycle and their impact on the global deepwater circulation, *Paleoceanography*, *3*, 343–360, 1988.

Fanning, A. F., and A. J. Weaver, Temporal-geographical meltwater influences on the North Atlantic conveyor: Implications for the Younger Dryas, *Paleoceanography*, *12*, 307–320, 1997.

Ganopolski, A., and S. Rahmstorf, Rapid changes of glacial climate simulated in a coupled climate model, *Nature*, *409*,153–158, 2001.

Ganopolski, A., S. Rahmstorf, V. Petoukhov, and M. Claussen, Simulation of modern and glacial climates with a coupled global model of intermediate complexity, *Nature*, *391*, 351–356, 1998.

Hostetler, S. W., and A. C. Mix, Reassessment of ice-age cooling of the tropical ocean and atmosphere, *Nature*, *399*, 673–676, 1999.

Imbrie, J., J. Hays, D. G. Martinson, A. McIntyre, A. C. Mix, J. J. Morley, N. G. Pisias, W. L. Prell, and N. J. Shackleton, The orbital theory of Pleistocene climate: Support from a revised chronology of the marine ^{18}O record, in *Milankovic and Climate*, edited by A. Berger et al., pp. 269–305. D. Reidel, Norwell, Mass., 1984.

Imbrie, J., A. McIntyre, and A. C. Mix, Oceanic response to orbital forcing in the late Quaternary: Observational and experimental strategies, in *Climate and Geosciences, A Challenge for Science and Society in the 21st Century*, edited by A. Berger, S. H. Schneider, and J.-C. Duplessy, pp. 121–164, Kluwer Acad., Norwell, Mass., 1989.

Imbrie, J., et al., On the structure and origin of major glaciation cycles, 1, Linear responses to Milankovitch forcing, *Paleoceanography*, *7*, 701–738, 1992.

Latif, M., Tropical Pacific/Atlantic Ocean interactions at multi-decadal time scales, *Geophys. Res. Lett.*, *28*, 539–542, 2001.

Latif, M., E. Roeckner, U. Mikolajewicz, and R. Voss, Tropical stabilization of the thermohaline circulation in a greenhouse warming simulation, *J. Clim.*, *13*, 1809–1813, 2000.

Lea, D., D. Pak, and H. Spero, Climate impact of late Quaternary equatorial Pacific sea surface temperature variations, *Science*, *289*, 1719–1724, 2000.

Levitus, S., R. Burgett, and T. P. Boyer, *World Ocean Atlas 1994*, vol. 3, *Salinity, NOAA Atlas NESDIS 3*, Natl. Oceanic and Atmos. Admin., 1994.

Licciardi, J. M., P. U. Clark, J. W. Jenson, and D. R. MacAyeal, Deglaciation of a soft-bedded Laurentide ice sheet, *Quat. Sci. Rev.*, *17*, 427–448, 1998.

Lohmann, G., and S. Lorenz, On the hydrological cycle under paleoclimatic conditions as derived from AGCM simulations, *J. Geophys. Res.*, *105*, 17,417–17,436, 2000.

Lohmann, G., R. Voss, and U. Mikolajewicz, On the global water cycle and the thermohaline circulation: Analysis of a coupled general circulation model, *Atmos. Ocean*, in press, 2001.

Manabe, S., and R. J. Stouffer, Simulation of abrupt climate change induced by freshwater input to the North Atlantic Ocean, *Nature*, *378*, 165–167, 1995.

Manabe, S., and R. J. Stouffer, Are two modes of thermohaline circulation stable?, *Tellus, Ser. A*, *51*, 400–411, 1999.

Mikolajewicz, U., T. J. Crowley, A. Schiller, and R. Voss, Modelling teleconnections between the North Atlantic and North Pacific during the Younger Dryas, *Nature*, *387*, 384–387, 1997.

Moore, T. C., J. C. G. Walker, D. K. Rea, C. F. M. Lewis, L. C. K. Shane, and A. J. Smith, Younger Dryas interval and outflow from the Laurentide ice sheet, *Paleoceanography*, *15*, 4–18, 2000.

Peltier, W. R., Postglacial variations in the level of the sea: Implications for climate dynamics and solid-earth geophysics, *Rev. Geophys.*, *36*, 603–689, 1998.

Rahmstorf, S., Bifurcations of the Atlantic thermohaline circulation in response to changes in the hydrological cycle, *Nature*, *378*, 145–149, 1995.

Rahmstorf, S., On the freshwater forcing and transport of the Atlantic thermohaline circulation, *Clim. Dyn.*, *12*, 799–811, 1996.

Ruddiman, W. F., and A. McIntyre, Oceanic mechanisms for amplification of the 23,000-year ice-volume cycle, *Science*, *212*, 617–627, 1981.

Rühlemann, C., S. Mulitza, P. J. Müller, G. Wefer, and R. Zahn, Warming of the tropical Atlantic Ocean and slowdown of thermohaline circulation during the last deglaciation, *Nature*, *402*, 511–514, 1999.

Schiller, A., U. Mikolajewicz, and R. Voss, The stability of the thermohaline circulation in a coupled ocean-atmosphere general circulation model, *Clim. Dyn.*, *13*, 325–347, 1997.

Schmittner, A., and T. F. Stocker, The stability of the thermohaline circulation in global warming experiments, *J. Clim.*, *12*, 1117–1133, 1999.

Schmittner, A., and T. F. Stocker, A seasonally forced ocean-atmosphere model for paleoclimate studies, *J. Clim.*, *14*, 1055–1068, 2001.

Schmittner, A., C. Appenzeller, and T. F. Stocker, Enhanced Atlantic freshwater export during El Niño, *Geophys. Res. Lett.*, *27*, 1163–1166, 2000.

Schmittner, A., M. Yoshimori, and A. J. Weaver, Instability of glacial climate in an Earth System Climate Model, *Science*, *295*, 1493–1498, 2002.

Stocker, T. F., The seasaw effect, *Science*, *282*, 61–62, 1998.

Stocker, T. F., and D. G. Wright, Rapid transitions of the ocean's deep circulation induced by changes in surface water fluxes, *Nature*, *351*, 729–732, 1991.

Stocker, T. F., and D. G. Wright, Rapid changes in ocean circulation and atmospheric radiocarbon, *Paleoceanography*, *11*, 773–796, 1996.

Stocker, T. F., D. G. Wright, and L. A. Mysak, A zonally averaged, coupled ocean-atmosphere model for paleoclimate studies, *J. Clim.*, *5*, 773–797, 1992.

Talley, L. D., Distribution and formation of North Pacific Intermediate Water, *J. Phys. Oceanogr.*, *23*, 517–537, 1993.

van Geen, A., R. G. Fairbanks, P. Dartnell, M. McGann, J. V. Gardner, and M. Kashgarian, Ventilation changes in the northeast Pacific during the last deglaciation, *Paleoceanography*, *11*, 519–528, 1996.

Venz, K. A., D. A. Hodell, C. Stanton, and D. A. Warnke, A 1.0 Myr record of Glacial North Atlantic Intermediate Water variability from ODP site 982 in the northeast Atlantic, *Paleoceanography*, *14*, 42–52, 1999.

Warren, B. A., Why no deep water formed in the North Pacific, *J. Mar. Res.*, *41*, 327–347, 1983.

Weaver, A. J., M. Eby, A. F. Fanning, and E. C. Wiebe, Simulated influence of carbon dioxide, orbital forcing and ice sheets on the climate of the Last Glacial Maximum, *Nature*, *394*, 847–853, 1998.

Weaver, A. J., C. M. Bitz, A. F. Fanning, and M. M. Holland, Thermohaline circulation: High latitude phenomena and the difference between Pacific and Atlantic, *Annu. Rev. Earth Planet. Sci.*, *27*, 231–285, 1999.

Weyl, P. K., The role of the oceans in climate change: A theory of the ice ages, *Meteorol. Monogr.*, *8*, 37–62, 1968.

Winguth, A. M. E., D. Archer, J.-C. Duplessy, E. Maier-Reimer, and U. Mikolajewicz, Sensitivity of paleonutrient tracer distributions and deep-sea circulation to glacial boundary conditions, *Paleoceanography*, *14*, 304–323, 1999.

Wright, D. G., and T. F. Stocker, A zonally averaged ocean model for the thermohaline circulation, part I, Model development and flow dynamics, *J. Phys. Oceanogr.*, *21*, 1713–1724, 1991.

Wright, D. G., and T. F. Stocker, Younger Dryas experiments, in *Ice in the Climate System, NATO ASI Ser., Ser. I*, vol. 12, edited by W. R. Peltier, pp. 395–416, Springer-Verlag, New York, 1993.

Yasuda, I., The origin of North Pacific Intermediate Water, *J. Geophys. Res.*, *102*, 893–909, 1997.

Zahn, R. J., H. R. Kudrass, M. H. Park, H. Erlenkeuser, and P. Gootes, Thermohaline instability in the North Atlantic during meltwater events: Stable isotope and ice-rafted detritus records from core SO75-26KL, Portugese margin, *Paleoceanography*, *12*, 696–710, 1997.

Zebiak, S. E., and M. A. Cane, A model El Niño–Southern Oscillation, *Mon. Weather Rev.*, *115*, 2262–2278, 1987.

Zheng, Y., A. van Geen, R. F. Anderson, J. V. Gardner, and W. E. Dean, Intensification of the northeast Pacific oxigen-minimum zone during the Bölling Alleröd warm period, *Paleoceanography*, *15*, 528–536, 2000.

A. C. Clement, University of Miami, Rosenstiel School of Marine and Atmospheric Science, Division of Meteorology and Physical Oceanography, 4600 Rickenbacker Causeway, Miami, FL 33149, USA. (aclement@rsmas.miami.edu)

A. Schmittner, School of Earth and Ocean Sciences, University of Victoria, P.O. Box 3055, Stn CSC, Victoria, British Columbia, V8W 3P6, Canada. (andreas@ocean.seos.uvic.ca)

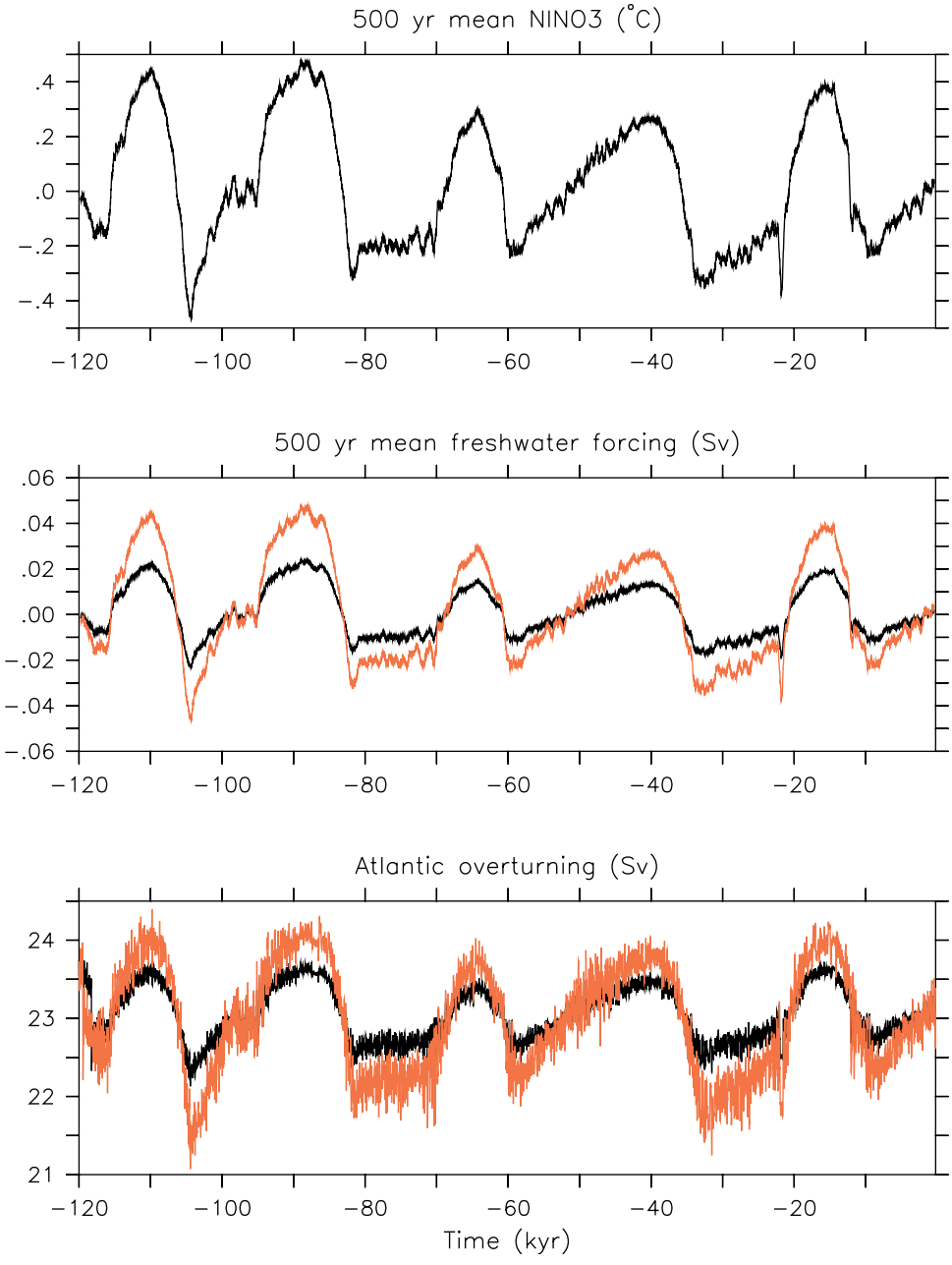

Figure 2. Time series of (top) NINO3 index, (middle) tropical freshwater forcing (positive values correspond to freshwater transfer from the Atlantic to the Pacific), and (bottom) response of the North Atlantic THC as annual mean maximum overturning below 1000 m depth. The black line corresponds to a small value for the coupling constant (m = 0.05 Sv K^{-1}; experiment LFHS; see (1) and Table 1), and the red line corresponds to a large value (m = 0.1 Sv K^{-1}; experiment HFHS).